CHAPTER 45

NUMERICAL MODELLING OF TROPICAL CYCLONE STORM SURGE

by

Rodney J. Sobey[1]
Bruce A. Harper[2]
George M. Mitchell[3]

ABSTRACT

Details are presented of a general numerical hydrodynamic model for the generation and propagation of tropical cyclone or hurricane storm surge. The model, known as SURGE, solves the two-dimensional depth-integrated form of the Long Wave Equations using an explicit finite difference procedure, with tropical cyclone surface wind and pressure forcing estimated from an adaption of available models based on U.S. hurricanes. Variations in tropical cyclone parameters as well as the physical characteristics of a coastal location such as bathymetry and details of capes, bays, reefs and islands are accommodated by the model. The accuracy and stability of the numerical solution have been confirmed by a comprehensive wave deformation analysis including quasi-non-linear effects and the open boundary problem has been overcome by the use of a Bathystrophic Storm Tide approximation to boundary water levels. A detailed sensitivity analysis has identified the principal surge generating parameters and the model has been checked against an historical tropical cyclone storm surge. SURGE has been used extensively in the northern Australian region and examples are presented.

INTRODUCTION

The tropical cyclone or hurricane storm surge is a meteorologically forced long wave motion resulting in a sustained superelevation of the sea surface, at least for a few hours, above that produced by the normal periodic astronomical tide. It is the result of the combined action on the underlying water body of the extreme atmospheric pressure gradients and wind shear stresses generated by a mature tropical cyclone. The region of surge intensification can extend over a substantial length of coastline (of order 200 km) and the development and impact of the surge wave at a particular site is sensitive to a number of meteorological and topographical factors. Briefly these are the intensity and scale of the tropical cyclone, the speed and track of the storm, the underwater and overbank terrain, offshore reefs and islands, local coastal features

1. Senior Lecturer, Department of Civil and Systems Engineering, James Cook University, Townsville 4811, Australia.
2. Engineer, Hydraulics Laboratory, N.S.W. Public Works Department, Manly Vale 2093, Australia.
3. Research Dynamicist, Atkins Research and Development, Epsom, Surrey KT18 5BW, United Kingdom.

(bays, headlands, estuaries) and the astronomical tide. Historically, storm tides have resulted in considerable damage to exposed coastlines, the flooding of low lying land and loss of life. A potentially critical situation arises when the total sustained water level (surge + tide) exceeds the highest astronomical tide (HAT) level.

In response to the need for reliable storm surge estimates in northern Australia for the design of coastal structures and for the protection of coastal communities, a numerical hydrodynamic model was developed within the Department of Civil and Systems Engineering at James Cook University. The model, known as SURGE, is a general numerical hydrodynamic model for the generation and propagation of tropical cyclone storm surge and can be applied to most coastal regions (12). It includes the effects of undersea bathymetry, offshore islands, reefs and other coastal features, as well as the flooding of low lying land. Tropical cyclone size, intensity and track can be varied continuously throughout a simulation to produce water flow patterns, contours of water level, coastal surge profiles at any time and water level and flow velocity time histories anywhere within the model area. SURGE is a comprehensive software system and is fully documented in the form of a user's guide (3). Particular attention has been given to the quite considerable problems of input data format and especially output data selection and presentation.

While numerical modelling of long wave propagation is not new, there are a number of unique aspects of the storm surge problem. In particular, the complex character and geophysical extent of the meteorological forcing, the specification of suitable open boundary conditions and the satisfactory resolution of the storm structure in discretised form all require special attention (12).

MATHEMATICAL FORMULATION

The response of a homogeneous sea to the meteorological forcing of a tropical cyclone is described by the full Navier-Stokes Equations for a homogeneous, incompressible fluid. Direct numerical solutions of these equations are as yet not feasible and a three-dimensional solution would only appear necessary where fluid density difference and/or the vertical flow structure may be important. An adequate description of long wave propagation (astronomical tides and storm surge) can be had from a two-dimensional vertically integrated form of the Reynolds Equations - the Long Wave Equations (17). These equations represent the conservation of mass and the conservation of momentum in horizontal directions x and y and time t:

$$\frac{\partial \eta}{\partial t} + \frac{\partial U}{\partial x} + \frac{\partial V}{\partial y} = 0 \tag{1}$$

$$\frac{\partial U}{\partial t} + \frac{\partial}{\partial x}\left(\frac{U^2}{\eta-d}\right) + \frac{\partial}{\partial y}\left(\frac{UV}{\eta-d}\right) - fV = -g(\eta-d)\frac{\partial \eta}{\partial x} - \left(\frac{\eta-d}{\rho_w}\right)\frac{\partial p_s}{\partial x} + \frac{1}{\rho_w}(\tau_{sx}-\tau_{bx}) \tag{2}$$

$$\frac{\partial V}{\partial t} + \frac{\partial}{\partial x}\left(\frac{UV}{\eta-d}\right) + \frac{\partial}{\partial y}\left(\frac{V^2}{\eta-d}\right) + fU = -g(\eta-d)\frac{\partial \eta}{\partial y} - \left(\frac{\eta-d}{\rho_w}\right)\frac{\partial p_s}{\partial y} + \frac{1}{\rho_w}(\tau_{sy}-\tau_{by}) \tag{3}$$

The x-y datum plane is located at the mean water level with the z axis directed vertically upwards. The water surface elevation with respect to datum is $\eta(x,y,t)$, the sea bed is $d(x,y)$ with respect to datum, U and V are depth-integrated flows per unit width, f is the Coriolis parameter and ρ_w is the mass density of sea water. The forcing influence of the tropical cyclone is represented through the surface wind shear stress vector $\underline{\tau}_s(x,y,t)$, resolved into components τ_{sx} and τ_{sy}, and the x and y gradients of the M.S.L. atmospheric pressure $p_s(x,y,t)$. The effect of bottom stress is represented through the seabed shear stress vector $\underline{\tau}_b(x,y,t)$, resolved into components τ_{bx} and τ_{by} such that, for example, in blue water regions:

$$\tau_{bx} = \frac{\lambda}{8}\,\rho_w\,\frac{|Q|U}{(\eta-d)^2} \tag{4}$$

where $Q = (U^2+V^2)^{\frac{1}{2}}$ and λ is the Darcy-Weisbach friction factor, assumed depth-dependent according to the Colebrook-White formula for a hydraulically rough boundary layer. Modified values of λ are adopted near reefs and for overbank flooding, the details being presented below.

At this stage the equations are sometimes linearised, neglecting the (normally small) convective accelerations. In SURGE all terms have been retained as they present no particular numerical problems and in some cases the commonly neglected terms (such as Coriolis and convective accelerations) can even be relatively important (5,12). A SURGE input option however does allow the convective terms to be omitted (3).

NUMERICAL SOLUTION

The flow field, coastal details, offshore and overbank bathymetry and coral reefs are represented on a square grid of unit dimension Δs and discrete values of the variables are specified on a space (x,y) and time (t) staggered computational grid, whose node points are defined as $(i\Delta x, j\Delta y, n\Delta t)$. Water surface elevation H (or η), bed elevation D (or d) with respect to M.S.L. and barometric head $B = p_s/\rho_w g$ are located at points (i,j,n), depth-integrated flow U and the surface wind shear stress term $WX = \tau_{sx}/\rho_w$ at $(i+\frac{1}{2},j,n+\frac{1}{2})$ and the depth-integrated flow V and the surface wind shear stress term $WY = \tau_{sy}/\rho_w$ at $(i,j+\frac{1}{2},n+\frac{1}{2})$ points.

Numerical integration of the partial differential Equations 1,2 and 3 is accomplished by an explicit "leapfrog" procedure similar to that used in the numerical simulation of storm tides in Galveston Bay, Texas, by Reid and Bodine (8). The computational molecules and explicit finite difference equations are listed in Table 1, the continuity equation being centred at $(i,j,n+\frac{1}{2})$, the x momentum equation at $(i+\frac{1}{2},j,n)$ and the y momentum equation at $(i,j+\frac{1}{2},n)$. In a number of special cases associated with boundary or internal (reef, weir, island) constraints, the complete finite difference Equations b and c of Table 1 cannot be implemented and suitably reduced forms (12) are adopted in such circumstances. Successive application of the x and y momentum equations and the continuity equation, together with appropriate boundary conditions advance the solution by one simulation time step Δt.

STABILITY AND WAVE DEFORMATION

As SURGE is based on explicit finite difference equations, numerical stability for all wave numbers is ensured only when the Courant number $Cr = (gA/b)^{\frac{1}{2}}\,\Delta t/\Delta x$ does not exceed unity.

TABLE 1. SURGE COMPUTATIONAL MOLECULES AND FINITE DIFFERENCE EQUATIONS

Mass Conservation Equation -

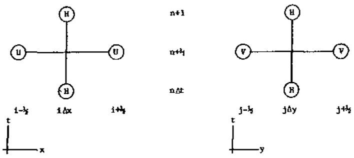

$$H^{n+1}_{i,j} = H^{n}_{i,j} - \left[\frac{U^{n+\frac{1}{2}}_{i+\frac{1}{2},j} - U^{n+\frac{1}{2}}_{i-\frac{1}{2},j}}{\Delta x} + \frac{V^{n+\frac{1}{2}}_{i,j+\frac{1}{2}} - V^{n+\frac{1}{2}}_{i,j-\frac{1}{2}}}{\Delta x}\right] \Delta t \qquad \text{(a)}$$

X Momentum Equation -

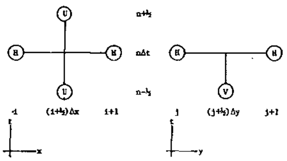

$$U^{n+\frac{1}{2}}_{i+\frac{1}{2},j} = [U^{n-\frac{1}{2}}_{i+\frac{1}{2},j}$$

$$- \{ \frac{U^{n-\frac{1}{2}}_{i+1\frac{1}{2},j}\ U^{n-\frac{1}{2}}_{i+1\frac{1}{2},j} / \overline{DX}^{n}_{i+1\frac{1}{2},j} - U^{n-\frac{1}{2}}_{i-\frac{1}{2},j}\ U^{n-\frac{1}{2}}_{i-\frac{1}{2},j} / \overline{DX}^{n}_{i-\frac{1}{2},j}}{2\Delta x}$$

$$+ \frac{U^{n-\frac{1}{2}}_{i+\frac{1}{2},j+1}\ \overline{\overline{V}}^{n-\frac{1}{2}}_{i+\frac{1}{2},j+1} / \overline{DX}^{n}_{i+\frac{1}{2},j+1} - U^{n-\frac{1}{2}}_{i+\frac{1}{2},j-1}\ \overline{\overline{V}}^{n-\frac{1}{2}}_{i+\frac{1}{2},j-1} / \overline{DX}^{n}_{i+\frac{1}{2},j-1}}{2\Delta y}$$

$$- \quad f\ \overline{\overline{V}}^{n-\frac{1}{2}}_{i+\frac{1}{2},j}$$

$$+ \quad g\ \overline{DX}^{n}_{i+\frac{1}{2},j} \frac{H^{n}_{i+1,j} - H^{n}_{i,j}}{\Delta x}$$

$$+ \quad g\ \overline{DX}^{n}_{i+\frac{1}{2},j} \frac{B^{n}_{i+1,j} - B^{n}_{i,j}}{\Delta x}$$

$$- \quad WX^{n}_{i+\frac{1}{2},j}\ \}\ \Delta t\ ] / [\ 1 + \Delta t\ \frac{\lambda}{8} \sqrt{(U^{n-\frac{1}{2}}_{i+\frac{1}{2},j})^2 + (\overline{\overline{V}}^{n-\frac{1}{2}}_{i+\frac{1}{2},j})^2} / (\overline{DX}^{n}_{i+\frac{1}{2},j})^2] \qquad \text{(b)}$$

where $\overline{DX}^{n}_{i+\frac{1}{2},j} = \frac{1}{2}(D_{i,j} + H^{n}_{i,j} + D_{i+1,j} + H^{n}_{i+1,j})$

$$\overline{\overline{V}}^{n-\frac{1}{2}}_{i+\frac{1}{2},j} = \frac{1}{4}(V^{n-\frac{1}{2}}_{i+1,j+\frac{1}{2}} + V^{n-\frac{1}{2}}_{i+1,j-\frac{1}{2}} + V^{n-\frac{1}{2}}_{i,j-\frac{1}{2}} + V^{n-\frac{1}{2}}_{i,j+\frac{1}{2}})$$

Y Momentum Equation -

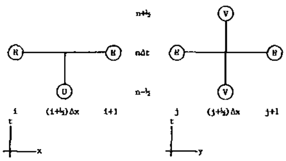

$$V^{n+\frac{1}{2}}_{i,j+\frac{1}{2}} = [V^{n-\frac{1}{2}}_{i,j+\frac{1}{2}}$$

$$- \{ \frac{\overline{\overline{U}}^{n-\frac{1}{2}}_{i+1,j+\frac{1}{2}}\ V^{n-\frac{1}{2}}_{i+1,j+\frac{1}{2}} / \overline{DY}^{n}_{i+1,j+\frac{1}{2}} - \overline{\overline{U}}^{n-\frac{1}{2}}_{i-1,j+\frac{1}{2}}\ V^{n-\frac{1}{2}}_{i-1,j+\frac{1}{2}} / \overline{DY}^{n}_{i-1,j+\frac{1}{2}}}{2\Delta x}$$

$$+ \frac{V^{n-\frac{1}{2}}_{i,j+1\frac{1}{2}}\ V^{n-\frac{1}{2}}_{i,j+1\frac{1}{2}} / \overline{DY}^{n}_{i,j+1\frac{1}{2}} - V^{n-\frac{1}{2}}_{i,j-\frac{1}{2}}\ V^{n-\frac{1}{2}}_{i,j-\frac{1}{2}} / \overline{DY}^{n}_{i,j-\frac{1}{2}}}{2\Delta y}$$

$$+ \quad f\ \overline{\overline{U}}^{n-\frac{1}{2}}_{i,j+\frac{1}{2}}$$

$$+ \quad g\ \overline{DY}^{n}_{i,j+\frac{1}{2}} \frac{H^{n}_{i,j+1} - H^{n}_{i,j}}{\Delta y}$$

$$+ \quad g\ \overline{DY}^{n}_{i,j+\frac{1}{2}} \frac{B^{n}_{i,j+1} - B^{n}_{i,j}}{\Delta y}$$

$$- \quad WY^{n}_{i,j+\frac{1}{2}}\ \}\ \Delta t\ ] / [\ 1 + \Delta t\ \frac{\lambda}{8} \sqrt{(\overline{\overline{U}}^{n-\frac{1}{2}}_{i,j+\frac{1}{2}})^2 + (V^{n-\frac{1}{2}}_{i,j+\frac{1}{2}})^2} / \overline{DY}^{n}_{i,j+\frac{1}{2}})^2\ ] \qquad \text{(c)}$$

where $\overline{DY}^{n}_{i,j+\frac{1}{2}} = \frac{1}{2}(D_{i,j} + H^{n}_{i,j} + D_{i,j+1} + H^{n}_{i,j+1})$

$$\overline{\overline{U}}^{n-\frac{1}{2}}_{i,j+\frac{1}{2}} = \frac{1}{4}(U^{n-\frac{1}{2}}_{i+\frac{1}{2},j+1} + U^{n-\frac{1}{2}}_{i+\frac{1}{2},j} + U^{n-\frac{1}{2}}_{i-\frac{1}{2},j} + U^{n-\frac{1}{2}}_{i-\frac{1}{2},j+1})$$

Compliance with this equation, however, does not necessarily guarantee the accuracy of the solution and a broader analysis of the model behaviour is necessary to fully examine the numerical distortion of the physical surge wave. Some measure of this distortion can be had from a comparison of the numerical and analytical solutions of the equations in the time domain using the complex propagation factor of Leendertse (6). This method allows evaluation of the wave-number-dependent amplitude and phase distortions introduced by the numerical solution.

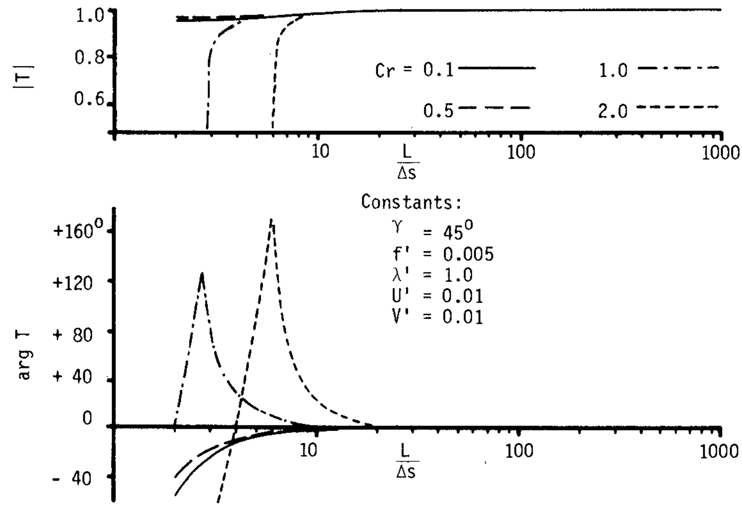

FIGURE 1. COMPLEX PROPAGATION FACTORS FOR COMPLETE QUASILINEAR FORM.

Assuming the non-linear interactions to be weak, as is generally the case for the Long Wave Equations, an evaluation of the wave deformation characteristics of the solution can be obtained from a quasilinear approximation to the finite difference equations (12). The complex propagation factor T is defined (6) as the ratio of the computed wave solution to the physical wave solution after a time interval in which the physical wave propagates over its wavelength L. Figure 1 shows the behaviour of $|T|$ and arg T for the complete quasilinear form of the Long Wave Equations with a constant wave propagation direction γ of 45^{o} and various values of Cr. Typical values of the non-dimensional parameters of the system,

$$U' = U_*\Delta t/D_*\Delta s \qquad f' = f\Delta t$$
$$V' = U_*\Delta t/D_*\Delta s \qquad \lambda' = \lambda\Delta s/8D_* \tag{5}$$

have been used to illustrate the solution behaviour. The starred variables U_*, V_* and D_* are constant and representative of the local flow field. The results show that the finite difference equations are appropriate discrete approximations to the partial differential equations across the complete wave number spectrum. For typical applications with Cr of 1.0 and L/Δs of order 25, negligible phase and amplitude distortion can be expected.

BOUNDARY CONDITIONS

The mathematical description of the computational field is completed by the specification of suitable boundary conditions, which for SURGE can be divided into a number of broad categories. Consistent with the staggered finite difference representation of the flow field, boundary conditions for either U or V (i.e. flow) situations take effect at spatial locations midway between nodes. For H (i.e. water level) situations the conditions require some interpretation in terms of the general finite difference equations; two or more conditions could apply at the one location and in many cases the spatial coverage of the general schemes needs to be restricted in the vicinity of a constraint. All this information is supplied to the model by the systematic specification of over fifty different flag conditions (3).

(a) *Coastal Boundaries*. These represent the simplest boundary conditions, stipulating vanishing normal transport across the coast at sea nodes adjacent to land nodes

$$\text{i.e.}\quad U^{n+\frac{1}{2}}_{i+\frac{1}{2},j} = 0 \qquad \text{or} \qquad V^{n+\frac{1}{2}}_{i,j+\frac{1}{2}} = 0 \tag{6}$$

Various combinations of these component conditions, together with the normal case of uninterrupted flow, allow the representation of any area of coastline.

(b) *Reefs and Low Barriers*. In terms of long wave propagation it is appropriate to represent the presence of reefs or sand banks within the flow field as a submerged broad-crested weir, an overflow broad-crested weir, or a total flow barrier. The exact representation depends upon the crest elevation of the reef z_{crest} with respect to the instantaneous water levels, H_u on the upstream side and H_d on the downstream side of the reef. This is shown schematically in Figure 2 where q is the resulting water discharge (i.e. U or V, depending on reef orientation) across the reef. In the vicinity of reefs it is convenient to omit the smaller convective and Coriolis acceleration terms from the momentum equations. The influence of the reef is then represented by an effective Darcy-Weisbach friction factor (7,13) based on the normal submerged and overflow broad-crested weir equations through an assumption of locally uniform flow:

$$\tau_{bx} = \frac{\lambda}{8}\,\rho_w\,\frac{|U|U}{(\eta-d)^2}$$

$$\text{where}\quad \lambda = \begin{cases} \dfrac{8(\eta-d)^2}{(C_1\Delta W_1)^2\,\Delta s} & \text{for submerged weir} \\[2ex] \dfrac{16(\eta-d)^3}{(C_2\Delta W_2)^2\,\Delta s} & \text{for over flow weir} \end{cases} \tag{7}$$

C_1 = submerged weir discharge coefficient ($\sqrt{2}$)
ΔW_1 = submerged weir head = $\frac{1}{2}(H_u + H_d) - z_{crest}$
C_2 = overflow weir discharge coefficient (0.5)
and ΔW_2 = overflow weir head = $H_u - z_{crest}$

For the case of $z_{crest} > H_u$ or H_d (total flow barrier), the conventional coastal boundary (a) applies. The continuity equation remains unchanged for all cases. For the representation of offshore reefs, the seabed levels ($D_{i,j}$) need not necessarily represent the selection for z_{crest} in regions where it is the subgrid effect which is being modelled. Such reef conditions have been used extensively for computations in the vicinity of the Great Barrier Reef.

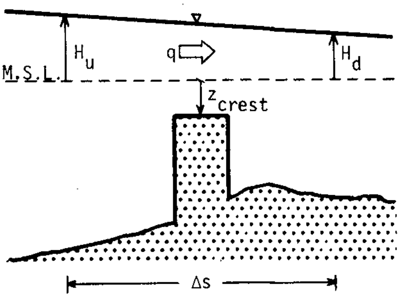

FIGURE 2. SCHEMATIC REPRESENTATION OF REEF BOUNDARY CONDITION.

(c) *Coastal Flooding.* The coastal flooding algorithm in SURGE represents the wetting and drying of low lying land through a two-dimensional cascade of broad-crested weirs and local storages (7,13). It is consistent in spirit with the representation of offshore reefs in (b). Each flood element is considered centred on a grid or H point and has horizontal dimensions Δs by Δs, with sides passing through the U and V locations at half-grid points. Bed elevation $D_{i,j}$ is as usual specified at the H point while broad-crested weirs with elevation $D_{i,j} + z_c|_{i,j}$ along all four sides totally surround each flood element. Adjacent elements have potentially different bed levels and crest elevations and at matching sides the higher of the two crest levels is considered operative in determining element exchange flows across that side, as illustrated in Figure 3a; this procedure was also followed for (b). The continuity equation is again unchanged, except that each element is constrained to empty only to the element crest level to characterise local pondage.

Frictional resistance to overbank flow is represented through the weir height z_c relative to local bed level and through the spacing of these weirs Δs. Given a grid scale, the choice of appropriate z_c, in the absence of calibration data, can reasonably be based on an engineering estimate of the equivalent weir behaviour of say urban housing or mangrove swamps. A non-dimensional weir friction diagram, Figure 3b, has been prepared to assist in the estimation and evaluation of overbank resistance. It is based on the λ estimates of Equation 7 and shows the dependence of the friction factor on the dimensionless relative weir height z_c/y_n, the dimensionless normal depth $y_n/\Delta s$ and the slope of the uniform flow energy grade line S, y_n being the normal depth.

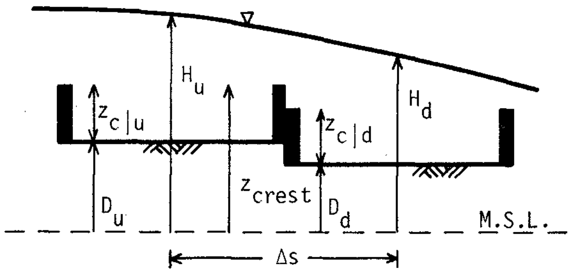

(a) Crest Elevation for Element Exchange Flow.

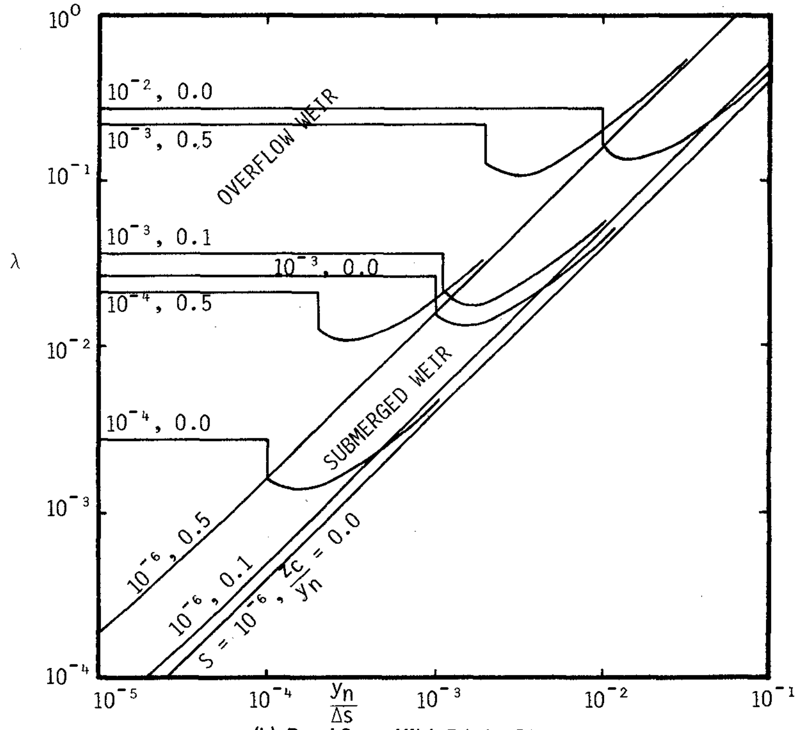

(b) Broad-Crested Weir Friction Diagram.

FIGURE 3. COASTAL FLOODING BOUNDARY CONDITION.

(d) *Open Sea Boundaries*. While open boundary conditions for *astronomical* tide propagation are quite straightforward and require only the specification of water surface histories at these locations for satisfactory representation, *meteorological* tides are generated by local surface forces. For a tropical cyclone the spatial extent of the forcing approaches 1000 km, although the region of peak positive and negative surges has a spatial scale of the order of the radius of maximum winds (typically 30 km). In such a case meteorological forcing outside the computational field can only be represented by the open boundary condition. Ideally the open boundaries would be insignificant. However, the storage and speed limitations of present time-shared computer systems preclude the adoption of a computational field that has linear dimensions of the order of 1000 km and simultaneously reproduces details on the scale of the radius of maximum winds. A practical compromise to this conflict of scales has been incorporated in SURGE by effectively including the forcing influence outside the computational field in the open boundary conditions.

Three separate forms of open boundary conditions are available in SURGE (11,12):

(i) Pressure Surge Condition ($H = \Delta B$), where open boundary water levels are set equal to the pressure surge, the head of water equivalent to the local atmospheric pressure deficit, i.e.

$$H^n_{i,j} = (p_\infty - p^n_s|_{i,j})/\rho_w g \tag{8}$$

This condition is regarded as only a first approximation to the actual water levels along an open boundary as it does not include the effects of the wind tide. The pressure surge condition is the default condition and is used as an initial value in condition (ii) below.

(ii) Bathystrophic Storm Tide (B.S.T.) Approximation, where open boundary water levels are set equal to the local bathystrophic storm tide, i.e. the quasi-steady profile described, for example by

$$0 = -g(\eta - d)\frac{\partial \eta}{\partial x} - \frac{(\eta - d)}{\rho_w}\frac{\partial p_s}{\partial x} + \frac{\tau_{sx}}{\rho_w} \tag{9}$$

when the open boundary is in the x direction and intersects the coastline.

From a physical viewpoint the bathystrophic tide condition provides a reasonably realistic boundary condition. It involves a lowest order momentum balance along the open boundary to include the forcing influence of the tropical cyclone outside the boundary. Water levels along the open boundary can rise and fall in response to the intensity and position of the tropical cyclone as shown in Figure 4. Such a boundary condition enables optimal use of the grid coverage, realistic water levels and flow patterns being obtained in close proximity to the boundaries. Detailed discussions are given elsewhere (11,12).

(iii) Time Dependent Water Level Inputs, where open boundary water levels are set equal to supplied water levels (e.g. tidal input, hydrographs),

$$H^n_{i,j} = h(t) \tag{10}$$

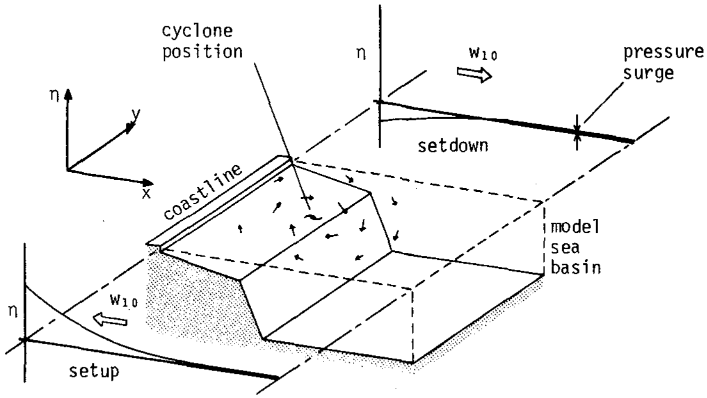

FIGURE 4. CONCEPT OF BATHYSTROPHIC STORM TIDE OPEN BOUNDARY CONDITION.

This form of open boundary condition can also be used in conjunction with (i) and (ii) above, although no interaction between the two inputs (e.g. meteorological and astronomical) is assumed. The appropriate meteorological forcing, pressure surge or B.S.T., is first applied with water levels at M.S.L., and the time dependent water levels are then added. Additionally this condition allows a "dual model" approach, in which water levels derived from a large scale model are used later as open boundary inputs to a smaller scale, detailed model of a particular section of coast.

TROPICAL CYCLONE FORCING

The aerodynamics of the tropical cyclone and the hydrodynamics of the underlying water body are coupled by the atmospheric pressure p_s and wind shear stress τ_s at the air-sea interface. Their estimation throughout the flow field during the passage of a tropical cyclone follows from the adoption of a suitable model of the near-surface meteorological structure of the storm. The model developed initially by Graham and Nunn (2,16) under the National Hurricane Research Project (NHRP) of the former U.S. Weather Bureau forms the basis of the tropical cyclone sub-model in SURGE. No claim is made that this model is entirely satisfactory; in fact our knowledge of tropical cyclone wind fields is far from complete, especially in Australia. It has been adopted in the absence of a more suitable alternative.

Many of the highly empirical aspects of the original NHRP model, such as rate of filling over land and the reduction of over-land wind speeds, have been omitted in favour of representing the major features of the tropical cyclone. In particular the radial wind and pressure profiles, the variation of the radial inflow angle and the asymmetry of the wind field are included and expressed in terms of the four parameters commonly assumed to characterise a tropical cyclone:

(i) Central pressure p_o at M.S.L.

(ii) Maximum sustained wind V_{10} at a height of 10 m above M.S.L.

(iii) Radius of maximum winds R.

(iv) Speed V_{FM} and direction θ_{FM} of storm forward movement.

SURGE allows all four parameters to be varied continuously to represent changes in storm intensity and track. Details may be found in Ref.12. Radial profiles of near-surface wind and M.S.L. atmospheric pressure are sketched in Figure 5a and Figure 5b shows a typical isovel and wind vector pattern for a moving model storm. The over-water wind speed W_{10} at height 10 m above M.S.L. and the resulting shear stress τ_s on the water surface are assumed to be related as

$$\tau_s = C_{10}\, \rho_a\, W_{10}{}^2 \tag{11}$$

where C_{10} is a non-dimensional surface friction or drag coefficient. Approximate relations for C_{10} over the range of wind speeds for oceanic applications according to W_u (18) are incorporated in SURGE.

MODEL VERIFICATION AND SENSITIVITY TESTING

Initial verification of the model hydrodynamics was accomplished by comparison of a numerical prediction with a known analytical solution for wind setup on a rectangular lake under constant wind forcing. The agreement was almost exact. Since analytical solutions more closely related to open coast tropical cyclone storm surge are not available, an alternative approach to detailed verification was adopted involving comparison with a documented record of an historical tropical cyclone storm surge (12).

The tropical cyclone ALTHEA storm surge near Townsville in December 1971 is probably the best documented storm surge to occur in Australia. Water level records from four automatic tide gauges (Mourilyan, Lucinda, Townsville and Bowen) plus post-cyclone debris level surveys enabled an order-of-magnitude reconstruction of the surge profile development along the coast. No flow velocity data was available, nor was there any record of water levels at other than coastal locations. The Bureau of Meteorology (1), with the aid of shore-based radar, traced the path of ALTHEA as it approached and crossed the continental shelf and estimated the meteorological parameters. The central pressure fell to 952 mb and the radius to maximum winds was typically 35 km. The storm crossed the coast approximately 45 km north of Townsville and registered a peak surge of 2.78 m above predicted tide level at Townsville Harbour.

The coastal region from Innisfail in the north to Bowen in the south and up to 260 km offshore was represented on a 5 n mile grid system of 30 by 40 points as shown in Figure 6 which includes the reconstructed path of ALTHEA. The coastline is shown as a series of straightline barriers while the Great Barrier Reef is indicated by a series of broken line barriers that maintain the recognised shipping passages. Due to an almost complete lack of information on the offshore astronomical tide, the simultaneous propagation of tide and surge could not be considered and the

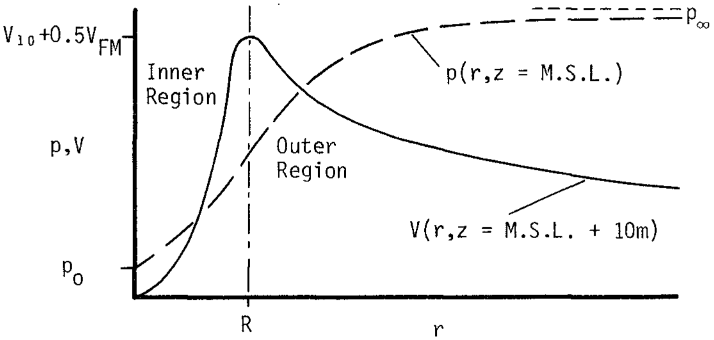

(a) Typical Wind Velocity and Atmospheric Pressure Profiles Along the Line of Maximum Winds.

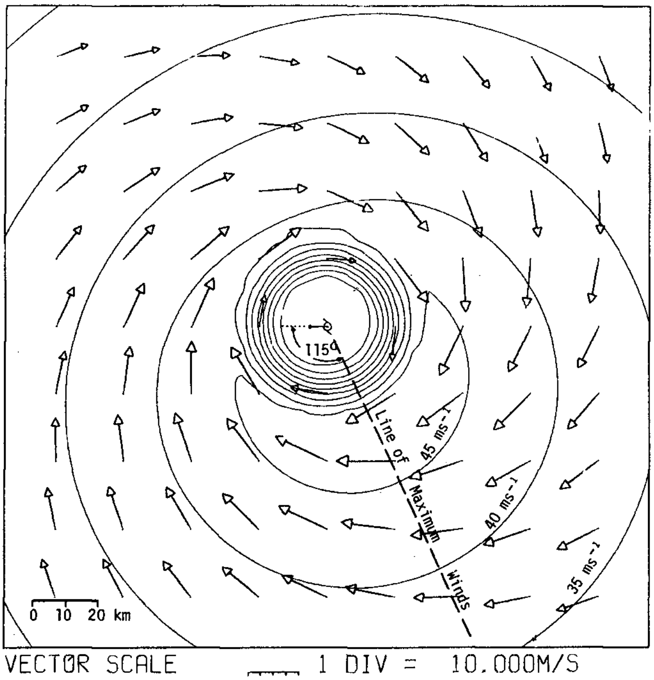

(b) Typical Isovel and Wind Vector Pattern for a Moving Model Storm

FIGURE 5. STRUCTURE OF TROPICAL CYCLONE FORCING.

hindcast is compared to the deviation of water levels away from predicted astronomical tide (and ignoring nonlinear interactions). Figures 7a and b show the results of the SURGE simulation compared with the storm surge hydrograph recorded at Townsville Harbour and also with less reliable data available on maximum coastal water levels. The results show good agreement with this limited historical record, even at this coarse 5 n mile resolution level. A more thorough evaluation will only be possible when spatially comprehensive time histories of sea surface development of the type promised by the SEASAT satellite programme become available. Figure 8a shows part of the model flow field shortly after the storm has crossed the line of barrier reefs and the strong currents generated along the coastline and through the numerous reef passages. Figure 8b shows contours of water level above M.S.L. at the time of storm landfall.

In addition to the comparison with an historical record, a comprehensive sensitivity analysis was undertaken to evaluate the model performance under various conditions (5,12) and to define the likely envelope of response. In particular, testing of various dynamic open boundary situations was undertaken together with consideration of bed friction specifications, bathymetry effects, coastal forms and initialization. A broad range of tropical cyclone parameters, including track, was also examined and highlighted the need for adequate resolution of the storm wind and pressure structure. An $R/\Delta s$ ratio of at least 4 was shown to be necessary for an accurate representation of the structure of the storm forcing.

MODEL APPLICATIONS

SURGE has been used extensively for the study of the tropical cyclone storm surge hazard in northern Australia. In particular a comprehensive analysis was undertaken for the Beach Protection Authority, Brisbane, at ten separate sites along the Queensland coast and covering over 2000 km of coastline (4,12). At each of the sties three tropical cyclones at each of three approach directions were modelled, based on a statistical analysis of historical tropical cyclone records, and their effect on coastal locations was examined in detail. This extensive study required the modelling of a wide range of coastal features from the shallow waters of the Gulf of Carpentaria, through the Great Barrier Reef dominated Coral Sea coast to the comparatively narrow and plunging continental shelf along Queensland's Gold Coast region. Other study areas in northern Australia include Mermaid Sound in Western Australia (14), an area subject to the most severe tropical cyclones in Australia, and even more detailed investigations of estuarine storm surge penetration at Weipa on Cape York Peninsula (15) and Trinity Inlet at Cairns (13). The latter two studies included the use of a one-dimensional hydrodynamic model ESTFLO (9) which was interfaced with SURGE. Figure 9 shows the Trinity Inlet model structure where a three-pass procedure was adopted, involving two successive grid scale reductions by factors of six and appropriate truncation of the computational field at each pass. This structure was necessary to include the area of significant meteorological forcing and still reproduce overbank flooding within Trinity Inlet and in a loop around Admiralty Island. This formulation was necessary to achieve a realistic representation of the flow pattern between the deeper channels which are the major vehicle for surge penetration, and the extensive mangrove areas. Figure 10 shows a typical time sequence of surge penetration and overbank flooding within the C grid region. Heights are in cm above M.S.L. datum.

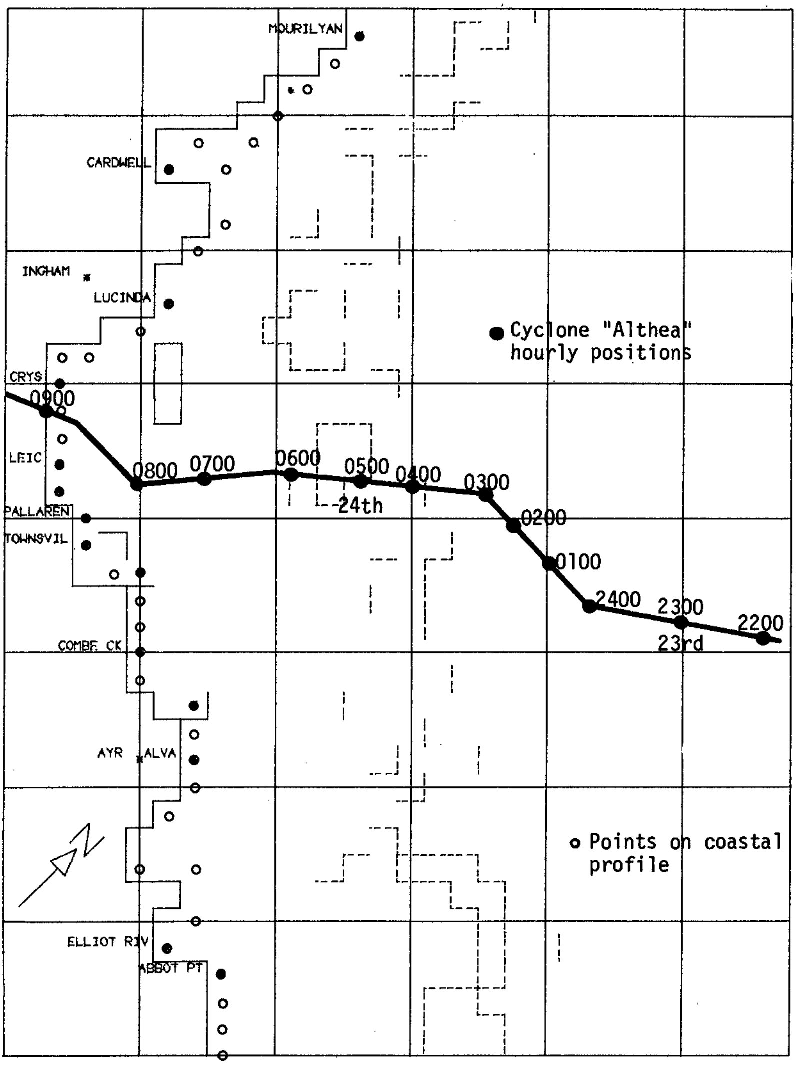

FIGURE 6. MODEL REPRESENTATION OF TOWNSVILLE REGION AND TRACK OF TROPICAL CYCLONE ALTHEA

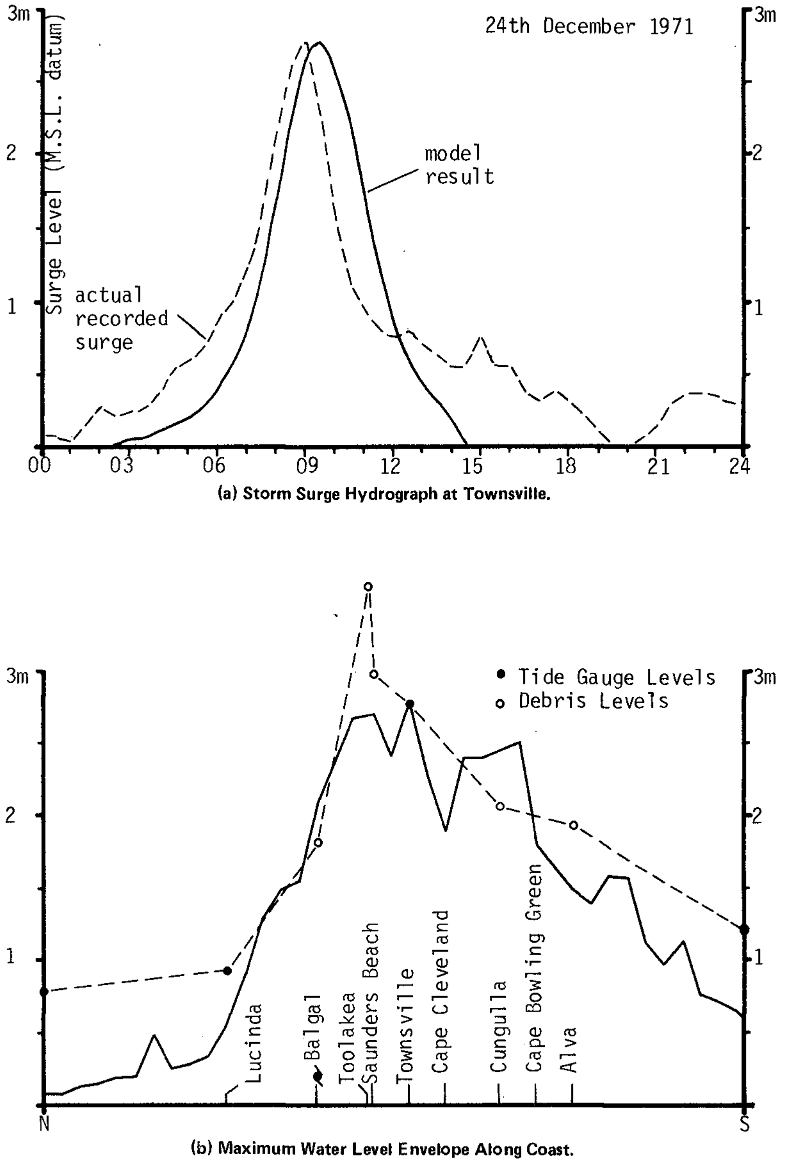

FIGURE 7. SURGE HINDCAST OF TROPICAL CYCLONE ALTHEA.

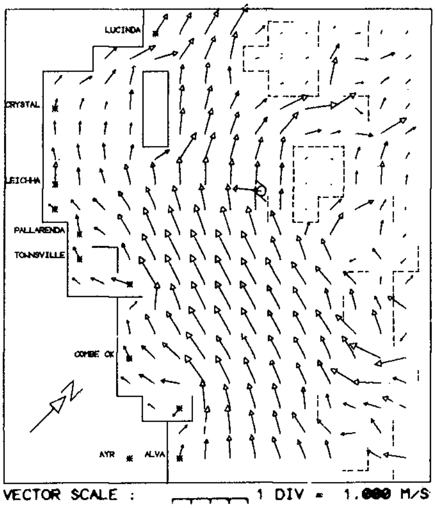

(a) Flow Velocity Pattern Three Hours before Storm Landfall.

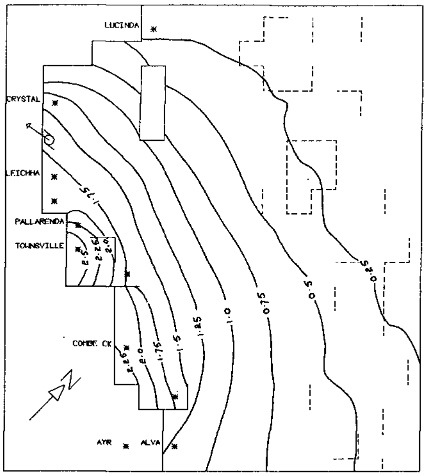

(b) Water Surface Contour Pattern at Time of Storm Landfall.

FIGURE 8. TYPICAL SURGE OUTPUT FOR ALTHEA HINDCAST.

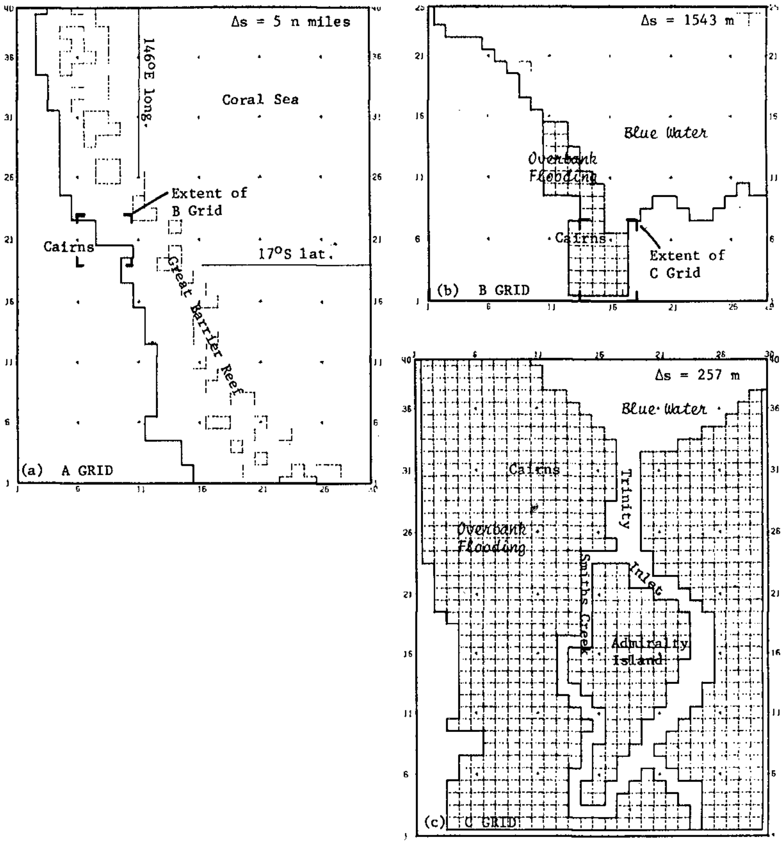

FIGURE 9. TRINITY INLET MODEL STRUCTURE.

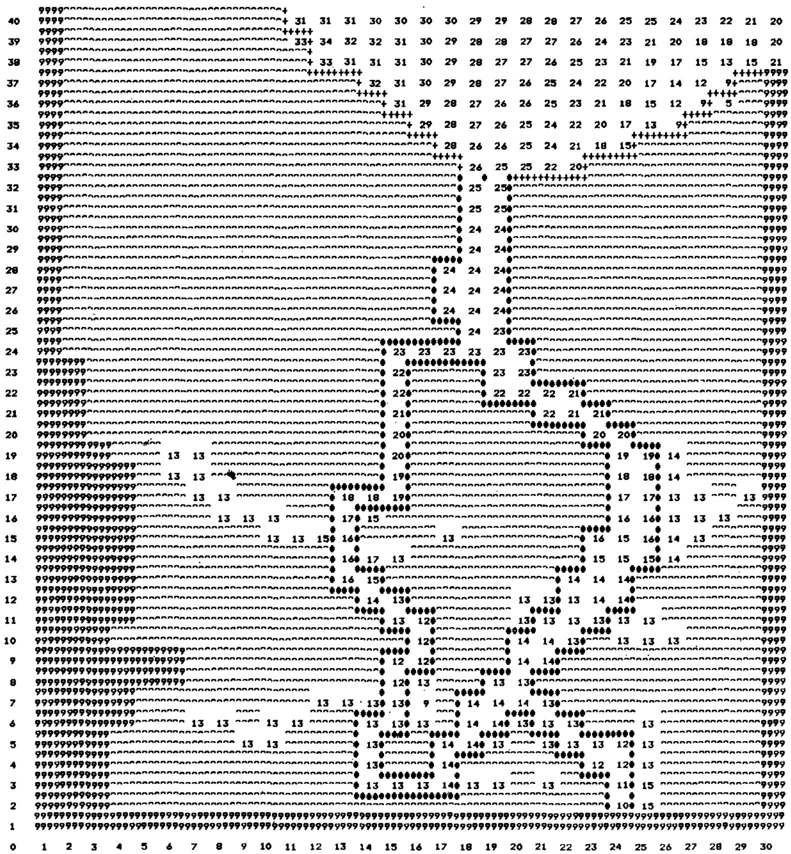

(a) Water Levels over C Grid One Hour before Storm Landfall.

FIGURE 10. OVERBANK FLOODING IN TRINITY INLET.

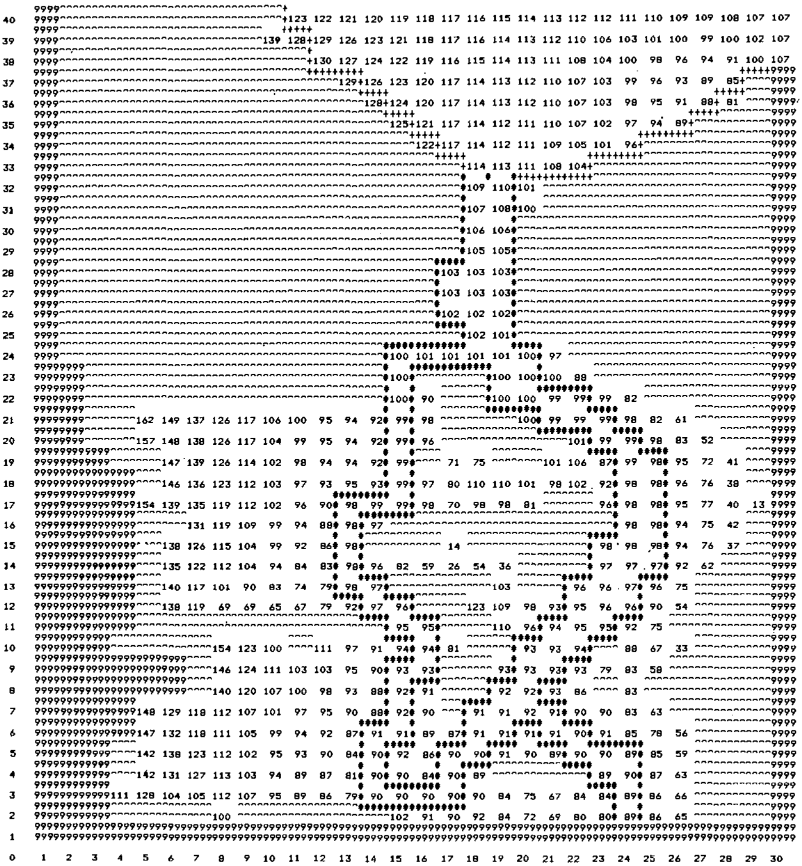

(b) Water Levels over C Grid at Storm Landfall.

FIGURE 10 (Continued). OVERBANK FLOODING IN TRINITY INLET.

CONCLUSIONS

The numerical hydrodynamic model SURGE adequately describes the generation and propagation of tropical cyclone storm surge and is sufficiently flexible to represent a wide range of coastal features and storm effects. Apart from applications in coastal engineering investigations, SURCE has a potential role, with improved weather monitoring, in providing real-time forecasting advice to aide in counter-disaster planning.

ACKNOWLEDGEMENTS

The authors wish to thank Professor K.P. Stark for his initiation and continued support of this programme of research. We also acknowledge contributions by colleagues T.S. Adil and A.B. Mills for overall model development. Financial support from the Beach Protection Authority, Brisbane, is gratefully acknowledged together with the kind permission of the Department of Housing and Construction, Canberra, for the use of some illustrations.

REFERENCES

1. Bureau of Meteorology, "Report by Director of Meteorology on Cyclone 'Althea'", July, 1972.
2. Craham, H.E. and Nunn, D.E., "Meteorological Considerations Pertinent to Standard Project Hurricane, Atlantic and Gulf Coasts of the United States", U.S. Weather Bureau, National Hurricane Research Project, Report No.33, 1959.
3. Harper, B.A., Sobey, R.J. and Stark, K.P., "User's Guide to SURGE", Department of Civil and Systems Engineering, James Cook University, November, 1977.
4. Harper, B.A., Sobey, R.J. and Stark, K.P., "Numerical Simulation of Tropical Cyclone Storm Surge along the Queensland Coast, Part I Weipa", Department of Civil and Systems Engineering, James Cook University, November, 1977 (for Beach Protection Authority, Brisbane). (Also Part II Cooktown, Part III Cairns, Part IV Innisfail, Part V Ingham, Part VI Townsville, Part VII Bowen, Part VIII Mackay, Part IX Rockhampton, Part X Gold Coast.)
5. Harper, B.A., Sobey, R.J. and Stark, K.P., "Sensitivity Analysis of a Tropical Cyclone Surge Model", in Noye B.J. (Editor) "Numerical Simulation of Fluid Motion", North-Holland, 1978, pp 371-381.
6. Leendertse, J.J., "Aspects of a Computational Model for Long Period Water-Wave Propagation", Rand Corporation, Santa Monica, RM-5294-PR, 1967.
7. Mitchell, G.M. and Sobey, R.J., "Coastal Flooding from Hurricane Storm Surge", Manuscript in preparation, 1980.
8. Reid, R.O. and Bodine, B.R., "Numerical Model for Storm Surges in Galveston Bay", Jnl. Waterways and Harbors Div., ASCE, 94, 1968, pp 33-57.
9. Sobey, R.J., Adil, T.S. and Vidler, P.F., "User's Guide to ESTFLO/Version 2B-A Numerical Hydrodynamic Model of Unsteady Gradually Varied Flow in a One-Dimensional, Well-Mixed Estuarine System", Department of Civil and Systems Engineering, James Cook University, February, 1980.
10. Sobey, R.J. and Harper, B.A., "Tropical Cyclone Surge Penetration Across the Great Barrier Reef", Procs., Third Australian Conference on Coastal and Ocean Engineering, I.E.Aust., Melbourne, 1977, pp 58-63.

11. Sobey, R.J. and Harper, B.A., "Open Boundary Conditions for Open Coast Hurricane Storm Surge", Manuscript in preparation, 1980.
12. Sobey, R.J., Harper, B.A. and Stark, K.P., "Numerical Simulation of Tropical Cyclone Storm Surge", Department of Civil and Systems Engineering, James Cook University, Research Bulletin No. CS14, May, 1977.
13. Sobey, R.J., Mitchell, G.M. and Adil, T.S., "Trinity Inlet Storm Surge Study", Department of Civil and Systems Engineering, James Cook University, May, 1979 (for Departmentof Housing and Construction, Melbourne).
14. Sobey, R.J., Mills, A.B. and Young, I.R., "Mermaid Sound Extreme Water Level Study", Department of Civil and Systems Engineering, James Cook University, May, 1979 (for Woodside Petroleum Development Pty. Ltd., Perth).
15. Sobey, R.J., Stark, K.P. and Adil, T.S., "Weipa Peninsula Extreme Water Level Study", Department of Civil and Systems Engineering, James Cook University, August, 1979 (for Comalco Ltd., Brisbane).
16. U.S. Weather Bureau, "Interim Report - Meteorological Characteristics of the Probable Maximum Hurricane, Atlantic and Gulf Coasts of the United States", Report No. HUR.7-97, 1968.
17. Welander, P., "Numerical Prediction of Storm Surges", Advances in Geophysics, 8, 1964, pp 315-379.
18. Wu, J., "Wind Stress and Surface Roughness at Air-Sea Interface", Jnl. Geophysical Research, 74, 1969, pp 444-455.